J. Phys. C: Solid State Phys., 16 (1983) 5995–6010. Printed in Great Britain

Localised canting models for substituted magnetic oxides

Carl E Patton and Yi-hua Liu†
Department of Physics, Colorado State University, Fort Collins, Colorado 80523, USA

Received 4 February 1983, in final form 14 June 1983

Abstract. A free energy formulation of localised canting in substituted magnetic oxides is described. In contrast with earlier attempts at mathematical formulations of localised canting, quantities which may be replaced by average values and those which must be considered on a site-to-site statistical basis are clearly delineated. In addition, the use of local canting to determine average split-sublattice molecular-field directions is done in an iterative self-consistent manner. The theoretical curves of magnetisation versus level of non-magnetic substituent are somewhat rounded, compared with the linear dependences which result from the Yafet–Kittel model. For a given ratio of exchange parameters, canting commences at somewhat lower substituent levels than from the Yafet–Kittel model. The curves are considerably less rounded than those from previous localised canting calculations.

Comparisons with experimental magnetisation data for YIG with Ge, Si, Zr, and Sc substitutions and for Li–Zn ferrite indicate several things: (*a*) no single exchange parameter can provide a good theoretical fit to the data for a given system over the full range of substitution; (*b*) the theoretical curves, when fitted to the data, indicate a decrease in the inter- to intrasublattice exchange integral ratio for large substitutions where canting effects become pronounced; (*c*) the fits, when based on the assumption of a randomly split sublattice and equal intra- and intersublattice interactions for the two parts of the split sublattice, are consistent with reported exchange constant ratios for the unsubstituted oxides. An additional comparison of theoretical incremental susceptibility values with data for Li–Zn ferrite reveals (*a*) a complete lack of agreement for a constant exchange ratio, and (*b*) fitted exchange parameters which decrease rapidly with increasing Zn substitution.

1. Introduction

Very soon after the first laboratory preparation of ferrite materials (see Verwey and Heilmann 1947) and the explanation of the magnetic moment in terms of the Néel (1948) two-sublattice model of ferrimagnetism, it was found that ferrites with more than a few tenths non-magnetic substituent atoms per formula unit showed significant departures from the Néel collinear model (Guillaud and Roux 1949, Guillaud and Creveaux 1950, Gorter 1950). Three theoretical strategies have been used in a continuing effort to explain these departures: (i) an exchange linkage approach in which the number of magnetic nearest neighbours determines whether a given magnetic ion will order, and hence contribute to the magnetisation (Néel 1950, Gilleo 1958); (ii) a uniform canting

† Visiting Research Associate on leave from the Department of Physics, Shandong University, People's Republic of China.

© 1983 The Institute of Physics

approach in which one sublattice is divided into two halves, each oppositely canted at some uniform canting angle relative to the average magnetisation (Yafet and Kittel 1952); and (iii) a localised canting approach in which individual moments on one sublattice are canted at different angles, depending on the specifics of the local magnetic environment (Geller *et al* 1962, 1964, Geller 1966, 1969, 1978).

A number of authors have attempted to make quantitative calculations using the above approaches. Gilleo (1960) used the exchange linkage approach and showed that one could obtain reasonable, semiquantitative agreement for the 0 K magnetisation and quantitative agreement for the Curie temperature of yttrium iron garnet (YIG) with octahedral substitution, based on the assumption that *d*-site iron ions with less than two *a*-site nearest neighbours act paramagnetically and do not contribute to the magnetic order. Néel (1950) had previously applied this same general idea to magnetisation data on zinc-substituted nickel ferrite. The Gilleo model was briefly applied to rare-earth iron garnets with good results (Geller 1960). Nowik (1968, 1969a) attempted to extend the Néel–Billeo approach by adding a third possible spin state, one with the iron moment antiparallel to the net magnetisation of its own sublattice. Geller (1969) has questioned the Nowik calculation on several points which generally relate to random spin canting.

Yafet and Kittel (1952) were the first to argue that non-magnetic substitutions on one sublattice could lead to a non-collinear or canted spin arrangement on the other sublattice. They developed a split-sublattice molecular field model to calculate a uniform canting angle θ_{YK}. A review of the Yafet–Kittel formulation is given in Appendix 1. Lotgering (1956) elaborated upon the Yafet–Kittel model to permit A-site canting, B-site canting, and antiferromagnetic sublattices, in addition to the usual ferrimagnetic order, and possible transitions between the various allowed combinations of the above states as a function of temperature.

De Gennes (1959) applied the Yafet–Kittel model to the then unpublished data of Geller and co-workers for YIG with *a*-site Sn^{4+} substitutions, assuming the split *d*-sublattices to be non-interacting. Such an assumption was reasonable, based on the original concept of *bona fide* split sublattices of a long-range nature. However, Anderson (1956) and Kaplan (1959, 1960) have argued that a Yafet–Kittel arrangement, if it exists at all, must be of a short-range nature. In the 1960s, Geller and co-workers developed a descriptive model of local random canting as mentioned above.

There have been five attempts to provide a mathematical framework for the random canting model of Geller and co-workers. Nowik (1969b) attempted to introduce localised canting into his previous three-spin-state model by making the *ad hoc* assumption that iron ions with only a single opposite-sublattice iron nearest neighbour were canted at some phenomenological canting angle. He also attempted to quantify Geller's (1969) idea of exchange constants which vary with the local magnetic environment. Rosencwaig (1970a, b) presented a localised variant of the Yafet–Kittel calculations in which nearest-neighbour exchange parameters were kept constant and local nearest-neighbour statistics were used to obtain local effective molecular fields and local canting angles. White *et al* (1979) extended the procedure by using the Rosencwaig average canting angle as a starting point in an iterative procedure to yield self-consistent local and average canting angles. Dickof *et al* (1980) have refined the Rosencwaig calculation by including next-nearest-neighbour considerations for spins on the sublattice experiencing canting. This leads to a fraction of such spins which undergo multiple reversals. A reasonable but still qualitative fit to data on zinc-substituted magnetite is obtained.

From the early work on substituted ferrites to the present, an increasing amount of magnetisation data, high-field susceptibility data, neutron diffraction data, and Möss-

bauer data support the concept of localised, random canting. Morrish (1981) has reviewed the experimental situation concerning hyperfine fields and implications for canted spin structures. A review of spin canting in garnets and models for its description has recently appeared in a review on magnetic garnets by Winkler (1981).

The objective of the present work is to provide a mathematical formulation of random localised canting, starting from a nearest-neighbour Heisenberg Hamiltonian, paying particular attention to those quantities which can be reasonably approximated by average values and those which cannot be so approximated. The formulation is self-consistent, in that local effective fields are used to evaluate average canting angles in an iterative manner until all fields are self-consistent. The model is presented and developed in §§ 2 and 3. Comparisons with experiment are made in § 4.

2. Free energy formulation

The Hamiltonian for the magnetic system, including nearest-neighbour Heisenberg terms of the form $-2J_{ij}\boldsymbol{S}_i \cdot \boldsymbol{S}_j$ and Zeeman terms is

$$H = -\sum_i \sum_{\text{NN to } i} J_{ij}\boldsymbol{S}_i \cdot \boldsymbol{S}_j - g\mu_B H_0 \sum_i S_{iz} \tag{1}$$

where the J_{ij} are the i–j nearest-neighbour exchange integrals, $\boldsymbol{S}_i$ and $\boldsymbol{S}_j$ are the spins on the i and j sites, g is the Landé g-factor, μ_B is the Bohr magneton, H_0 is the z-directed applied magnetic field, and S_{iz} designates the z-component of the spin $\boldsymbol{S}_i$ parallel to H_0. The free energy is now developed explicitly for yttrium iron garnet $Y_3Fe_5O_{12}$ with non-magnetic substitution on the octahedral a sites and canting of the Fe^{3+} spins on tetrahedral d sites. The model spin configuration is depicted in figure 1. In our notation, the two parts of the split d-sublattice are indicated as d' and d''.

Let the number of the three distinct Fe^{3+} magnetic ion species per formula unit be denoted by q_a, $q_{d'}$, and $q_{d''}$, respectively. Let the number of nearest-neighbour a-ions to an a-ion be denoted by n_{aa}, the number of nearest-neighbour d'-ions to an a-ion by $n_{ad'}$, and so on. The nine n parameters are given in table 1. The various q and n parameters will in general be a function of substituent level. With the Heisenberg exchange parameters all negative, sign problems are avoided by expressing all energies in terms of $|J_{aa}|$, $|J_{ad'}|$, $|J_{d'd''}|$, and so on. Note that $|S_a| = |S_{d'}| = |S_{d''}| = S$ is satisfied. Table 2 lists the twelve explicit free energy terms which follow from equation (1) for nearest-neighbour

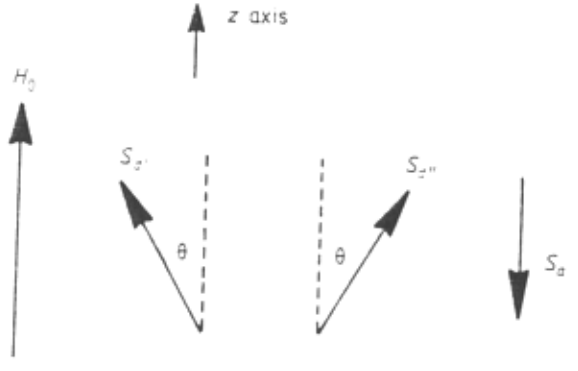

Figure 1. Model spin configuration for the free energy formulation of localised canting.

Table 1. Nearest-neighbour parameters.

Nearest-neighbour species	Central ion		
	a	d'	d''
a	n_{aa}	$n_{d'a}$	$n_{d''a}$
d'	$n_{ad'}$	$n_{d'd'}$	$n_{d''d'}$
d''	$n_{ad''}$	$n_{d'd''}$	$n_{d''d''}$

exchange and Zeeman interactions. The exchange integrals $J_{d'd'}$ $(=J_{d''d''})$ and $J_{d'd''}$ $(=J_{d''d'})$ *are for separate* d' and d'' Fe^{3-} nearest-neighbour pairs. As discussed in Appendix 2, the connection between the exchange parameters with primed subscripts and those with unprimed subscripts depends on the nature of the interaction between the two parts of the split sublattice.

The results of table 2 indicate a free energy of the form

$$E = A\cos\theta + B\cos(2\theta) + C. \tag{2}$$

With the assumption of equivalent d' and d'' split sublattices, the conditions $n_{ad'} = n_{ad''}$, $n_{d'a} = n_{d''a}$, and $q_{d'} = q_{d''}$ lead to the following coefficients in equation (2):

$$A = -2S^2[(q_a n_{ad'} + q_{d'} n_{d'a})|J_{ad'}| + g\mu_B H_0 q_{d'}/S], \tag{3}$$

$$B = 2S^2[q_{d'} n_{d'd''}]|J_{d'd''}|, \tag{4}$$

and

$$C = 2S^2[\tfrac{1}{2}q_a n_{aa}|J_{aa}| + q_{d'} n_{d'd'}|J_{d'd'}| + g\mu_B q_a H_0/2S]. \tag{5}$$

Given the above free energy results, a straightforward minimisation leads to an expression for a 'local' canting angle, θ_L. It is important to emphasise that θ_L constitutes a local canting angle for a d' or d'' Fe-ion moment only within the limited framework of our model. It is clear that for the random canting originally proposed by Geller and co-workers, any particular d' spin 'sees' a variety of d' and d'' nearest-neighbour spin orientations, not simply other d' and d'' spins at the same θ_L. From the above expressions

Table 2. Enumeration of energy terms.

Term	Energy
aa	$+\|J_{aa}\|q_a n_{aa} S^2$
ad'	$-\|J_{ad'}\|q_a n_{ad'} S^2\cos\theta$
ad''	$-\|J_{ad''}\|q_a n_{ad''} S^2\cos\theta$
$d'a$	$-\|J_{ad'}\|q_{d'} n_{d'a} S^2\cos\theta$
$d''a$	$-\|J_{ad''}\|q_{d''} n_{d''a} S^2\cos\theta$
$d'd'$	$+\|J_{d'd'}\|q_{d'} n_{d'd'} S^2$
$d''d''$	$+\|J_{d''d''}\|q_{d''} n_{d''d''} S^2$
$d'd''$	$+\|J_{d'd''}\|q_{d'} n_{d'd''} S^2\cos 2\theta$
$d''d'$	$+\|J_{d''d'}\|q_{d''} n_{d''d'} S^2\cos 2\theta$
$H_0 a$	$g\beta H_0 S q_a$
$H_0 d'$	$-g\beta H_0 S q_{d'}\cos\theta$
$H_0 d''$	$-g\beta H_0 S q_{d''}\cos\theta$

for A and B, $\cos\theta_L$ becomes

$$\cos\theta_L = \frac{(q_a n_{ad'} + q_{d'} n_{d'a})|J_{ad'}|S + g\mu_B H_0 q_{d'}}{4q_{d'} n_{d'd''}|J_{d'd''}|S}. \tag{6}$$

This expression is for a *local* canting angle θ_L which depends on the nearest-neighbour parameters $n_{d'a}$, $n_{ad'}$, and $n_{d'd''}$ at a particular site.

We close this section by making several observations about the formulation of Rosencwaig (1970a) as it relates to the above results. First, the average canting angle obtained from equation (6) by replacing the n parameters by their average values and observing that $q_a\langle n_{ad'}\rangle = q_{d'}\langle n_{d'a}\rangle$ is satisfied for garnets with a-site substitutions is

$$\cos\theta_{L\text{-}AV} = \langle n_{da}\rangle|J_{ad'}|/\langle n_{dd}\rangle|J_{d'd''} \tag{7}$$

for zero field. The corresponding expression, Rosencwaig's equation (5), is a factor of two smaller. This might be due to a failure to include both $J_{d'd''}S_{d'}\cdot S_{d''}$ and $J_{d''d'}S_{d''}\cdot S_{d'}$ energy terms in the free energy *or* the use of the de Gennes condition $J_{d'd''} = 2J_{dd}$ as discussed in Appendix 2. The second observation involves Rosencwaig's use of $2q_{d'}n_{d'a}$ rather than $(q_a n_{ad'} + q_{d'} n_{d'a})$ in determining local canting angles. While this replacement is valid when average $\langle n\rangle$ parameters are used, it is not accurate for strictly local calculations. This is easily seen by way of example. For a-substituted YIG, $n_{d'a}$ can range from zero to four while $n_{ad'}$ will be equal to three for any a-site Fe^{3+} ion. Thus $(q_a n_{ad'} + q_{d'} n_{d'a})$ can range from $(3q_a)$ to $(3q_a + 4q_{d'})$ while $2q_{d'}n_{d'a}$ will range from zero to $8q_{d'}$. For $q_a = 2 - x$ and $q_{d'} = 1.5$, these factors range from $6 - 3x$ to $12 - 3x$ for $(q_a n_{ad'} + q_{d'} n_{d'a})$ and from zero to 12 for $2q_{d'}n_{d'a}$ as $n_{d'a}$ is varied from zero to four. In general, the canting on d-sites with few a-site Fe^{3+} ions will tend to be overestimated by the Rosencwaig replacement. Numerical comparisons indicate that the Rosencwaig replacement yields larger average canting angles than either the Yafet–Kittel model or the calculation presented here. The published curves of moment versus substituent level are much more rounded than those obtained from either Yaget–Kittel or the present theory.

3. Effective field formulation

It is useful to formulate the various interactions discussed in § 2 in terms of effective fields acting on the canted d'-sublattice spins. In doing so, however, it is important to consider the *total* free energy of the system.

For the problem at hand, the energy minimisation equation, $\partial E/\partial\theta = 0$, can be interpreted as an effective torque equation for a d' spin moment,

$$[(q_a n_{ad'} + q_{d'} n_{d'a})|J_{ad'}|S^2 + g\mu_B S H_0 q_{d'}]\sin\theta_L - [2q_{d'}n_{d'd''}|J_{d'd''}|S^2]\sin 2\theta_L = 0. \tag{8}$$

The first term has the appearance of a torque that results from an a-sublattice local effective field and the z-directed applied field at the d' site. From the energy origins of this term, it is clear that the d' and d'' sublattice local effective fields at an a site also contribute to this term. The second term looks like a torque from the d'' sublattice local effective field at a d' site (or vice versa). From § 2, however, it is clear that both d'–d'' *and* d''–d' energy terms contribute.

From the above, the following effective fields may be identified:

$$H_{d'a} = \frac{(q_a n_{ad'} + q_{d'} n_{d'a})|J_{ad'}|S}{g\mu_B q_{d'}}\hat{k}, \tag{9a}$$

$$\boldsymbol{H}_0 = H_0\hat{\boldsymbol{k}}, \tag{9b}$$

$$\boldsymbol{H}_{d'd''} = (2n_{d'd''}|J_{d'd''}|S/g\mu_B)(-\cos\theta_L\hat{\boldsymbol{k}} + \sin\theta_L\hat{\imath}). \tag{9c}$$

where $\hat{\imath}$ and $\hat{\boldsymbol{k}}$ denote unit vectors perpendicular or parallel to the static field respectively.

The above fields may be incorporated into an iterative calculation of the average canting angle and magnetisation. This procedure was implemented first by White *et al* (1979) and considers, as did Rosencwaig, the $n_{d'a}$ nearest-neighbour parameters on a site-by-site basis. For zinc in Li ferrite, as an example, $n_{B'A}$ ranges from 0 to 6. For scandium in YIG, $n_{d'a}$ ranges from 0 to 4. For each such value, $n_{d'a}$ (or $n_{B'A}$) = m, we have one explicit value of the effective field $H_{d'a}$, denoted by $H_{d'a}(m, x)$, with x indicating the amount of substitution of the non-magnetic species per formula unit. By way of

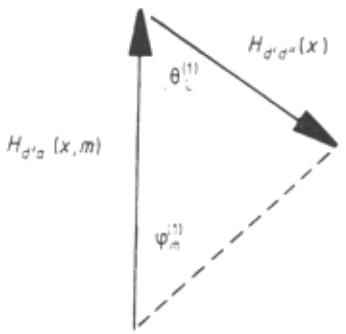

Figure 2. Effective field configuration for the localised, iterative canting calculation.

approximation, $n_{ad'}$ and $n_{d'd''}$ are set equal to their average values. This is reasonable because the d-sublattice has a substantial population of Fe^{3+} ions for the substitutions normally encountered and the weighted probabilities for low $n_{ad'}$ or $n_{d'd''}$ values in a rigorous statistical calculation are quite small. This approximation is not reasonable for $n_{d'a}$, insofar as this parameter can be small and have a large statistical probability at the same time, especially for large x-values. Therefore, we write

$$H_{d'a}(m, x) = \frac{[q_a(x)\langle n_{ad'}(x)\rangle + q_{d'}(x)m]|J_{ad'}|S}{g\mu_B q_{d'}(x)}. \tag{10}$$

This field is directed along positive z. The $d'd''$ effective field, given by equation (9c), is written as

$$H_{d'd''}(x) = 2\langle n_{d'd''}\rangle|J_{d'd''}|S/g\mu_B. \tag{11}$$

This field is oriented at the angle $\langle\theta_L\rangle$ with respect to the negative z axis, with $\langle\theta_L\rangle$ obtained iteratively as follows:

(i) In the first iteration, $\langle\theta_L\rangle$ is estimated from $\cos\theta_{L\text{-}AV}$ in the average nearest-neighbour approximation of equation (7). The fields are as shown in figure 2, with θ $\theta_L^{(1)} = \theta_{L\text{-}AV} = \cos^{-1}\theta_{L\text{-}AV}$. For each value of m, a value of $\cos\varphi_m^{(1)}$ is obtained.

$$\cos\varphi_m^{(1)} = \frac{H_{d'a}(m, x) - H_{d'd''}(x)\cos\theta_L^{(1)}}{[H_{d'a}^2(m, x) + H_{d'd''}^2(x) - 2H_{d'a}(m, x)H_{d'd''}(x)\cos\theta_L^{(1)}]^{1/2}}. \tag{12}$$

From this set of $\cos\varphi_m^{(1)}$ values, the average canting angle is recalculated:

$$\cos\theta_{\mathrm{L}}^{(2)} = \sum_{m=0}^{n_{d'a}^{\max}} P_{da}(m, x)\cos\varphi_m^{(1)}. \tag{13}$$

$$P_{da}(m, x) = (1.0 - x)^m x^{(n_{da}^{\max} - m)} \binom{n_{d'a}^{\max}}{m}. \tag{14}$$

$$\binom{n_{d'a}^{\max}}{m} = \frac{n_{d'a}^{\max}!}{m!(n_{d'a}^{\max} - m)!}. \tag{15}$$

In the above, $n_{d'a}^{\max}$ is the number of nearest-neighbour a sites for a given d' site.

(ii) The iterative strategy is evident from the above equations. One simply replaces $\cos\theta_{\mathrm{L}}^{(1)}$ by $\cos\theta_{\mathrm{L}}^{(2)}$ in equation (12), and recalculates a new set of $\cos\varphi_m^{(3)}$, and so on. As the $\cos\varphi_m^{(i)}$ converge to some unchanging set and $\cos\theta_{\mathrm{L}}^{(i)}$ converges to some value, the procedure is terminated. In this way a self-consistent set of local φ_m values and average $\theta_{\mathrm{L}}^{(\infty)}$ values are obtained. The magnetisation is then calculated from

$$|M| = M_d\cos\theta_{\mathrm{L}}^{(\infty)} - M_a. \tag{16}$$

By adding an applied field H_0 to $H_{d'a}(m, x)$ in equation (12), one can easily extend the calculation to obtain $M(H_0)$ and the incremental susceptibility $\chi = \mathrm{d}M/\mathrm{d}H_0$ as a function of field.

4. Comparison with experiment

In this section, experimental results for three classes of substitutions will be used as a basis for comparison of the model predictions. The first is YIG with a-sublattice substitutions of Sc and Zr (Geller *et al* 1964). The second is for YIG with d-sublattice substitutions of Ge and Se, from the same reference, hereafter referred to as GWES. The actual data points in both cases were transcribed from the figures in the Geller (1978) review. Finally, zinc-substituted lithium ferrite will be considered. Zinc enters the A sites in this spinel structure and canting occurs for B-site iron.

Figure 3 shows the experimental data points of GWES for Zr- and Sc-substituted YIG. The extrapolated 0 K magnetisation in units of Bohr magnetons (μ_{B}) per formula unit is shown as a function of substituent level x in at./formula unit. The site distributions of the various ions for these two systems are taken to be $\{Y_3\}[Sc_xFe_{2-x}](Fe_3)O_{12}$ and $\{Y_{3-x}Ca_x\}[Zr_xFe_{2-x}](Fe_3)O_{12}$, according to the usual nomenclature. The full curves in figure 3 indicate theoretical predictions based on the present model for various choices of the $J_{d'a}/J_{d'd''}$ ratio and appropriate q and $\langle n\rangle$ parameters for YIG with a-site substitutions. $\langle n_{d'a}\rangle = 2(2 - x)$, $\langle n_{ad'}\rangle = 3$, $\langle n_{d'd''}\rangle = 2$, $q_a = 2 - x$, and $q_{d'} = 1.5$. The upper straight line is the Yafet–Kittel prediction for $J_{d'a}/J_{d'd''} = 2$. The lower broken line will be discussed shortly.

The results in figure 3 show that the present theory yields somewhat rounded curves of magnetisation versus substituent level, and that the onset of canting is shifted to somewhat lower substituent concentrations than predicted by Yafet–Kittel for a given exchange ratio. The theoretical curves are much less rounded than those obtained by Rosencwaig. From these results, about the most that can be said is that $J_{d'a}/J_{d'd''}$ ratios between 1.5 and 1.75 appear to model the data best near the peak. No single ratio gives a reasonable overall fit. The results do suggest a $J_{d'a}/J_{d'd''}$ ratio which is decreasing at the higher substituent levels.

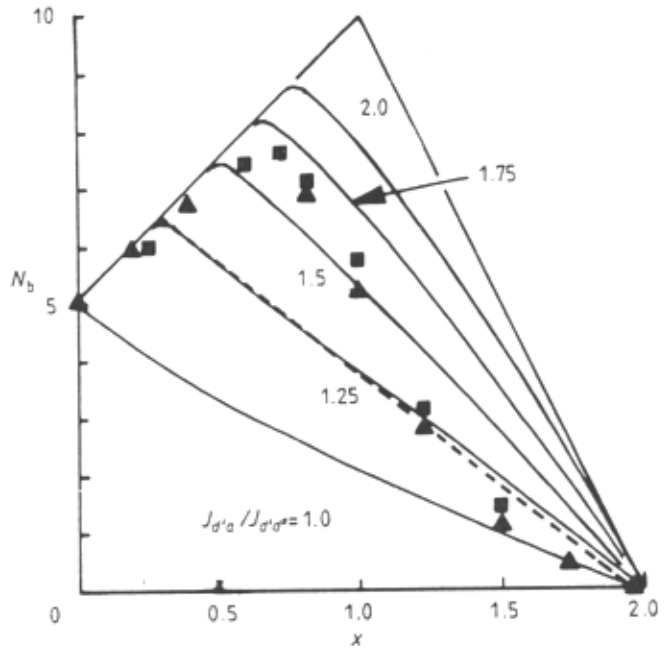

Figure 3. Comparison of theoretical predictions with data on the 0 K spontaneous moment of Zr- and Sc-substituted YIG by Geller *et al* (1964). The moment N_b in μ_B per formula unit is shown as a function of substituent level x in $\{Y_3\}[Sc_xFe_{2-x}](Fe_3)O_{12}$ (squares) and $\{Y_3\}[Zr_xFe_{2-x}](Fe_3)O_{12}$ (triangles).

It is of interest to compare the above results with literature estimates of the exchange integral ratios. Representative values are given in table 3 for J_{da}/J_{dd} and J_{ad}/J_{aa}. The latter ratio will be important for YIG with *d*-site substitution, to be considered next. In cases where molecular-field λ parameters were listed in the indicated citation, the conversion recipe given in Appendix 3 was used to obtain the appropriate exchange integral ratios. Numerous discrepancies occur in the literature concerning the actual

Table 3. Literature values of J_{da}/J_{dd} and J_{ad}/J_{aa} for yttrium iron garnet.

J_{da}/J_{dd}	J_{ad}/J_{aa}	Remarks
2.318	4.221	Pauthenet (1958), molecular-field theory fitted to magnetisation data versus temperature.
2.29	4.36	Douglass (1960), based on Pauthenet (1958) data.
2.434	4.120	Aléonard (1960), molecular-field theory fitted to high-temperature susceptibility data.
5.00	5.00	Harris (1963), based on fits to the magnetisation data of Solt (1962) and the measured spin-wave stiffness parameter.
2.349	4.229	Geller *et al* (1964), based on Pauthenet (1958) data.
2.138	3.001	Anderson (1964), based on molecular-field theory fitted to magnetisation data.
2.306	3.251	
9.758	—	Wojtowicz (1964), based on the high-temperature susceptibility
28.7	—	data of Aléonard (1960).
11.250	45.0	Gonano *et al* (1967), based on NMR data and fits to spin-wave
±2.86	±45.0	theory.
2.127	2.985	Dionne (1970), molecular-field theory filled to the magnetisation data versus temperature by Gilleo and Geller (1958).

exchange integrals, and the interested reader is urged to consult the original papers. Ratios are given to three places for purposes of comparison only.

In making comparisons between the results in figure 3 and table 3 (as well as subsequent comparisons), it is important to remember that the relations between d–d exchange parameters with primed subscripts and those with unprimed subscripts depend on the starting assumptions about the d'–d' and d'–d'' split-sublattice interactions. This point is developed in Appendix 2. For a randomly split d sublattice, we have $J_{d'd''} = J_{dd}$. For the de Gennes (1959) condition, an ordered split d sublattice with no d–d interaction, we have $J_{d'd''} = 2J_{dd}$. In both cases, $J_{d'a} = J_{da}$ is satisfied.

For a randomly split d sublattice, therefore, the 'best fit' ratio of 1.15–1.75 near the data maximum in figure 3 for $J_{d'a}/J_{d'd''}$ corresponds to a 'best fit' J_{da}/J_{dd} ratio of 1.5–1.75 as well. This ratio is somewhat below the ratios listed in table 3, which generally fall in the range 2–2.5. This comparison suggests a decrease in the J_{da}/J_{dd} ratio with increasing a-sublattice substitution. Such a decrease is consistent with the trend of the data in figure 3 for $x > 0.75$, which indicate (in comparison with the calculated curves) a rapid decrease in the J_{da}/J_{dd} ratio at high levels of a-sublattice substitution. These decreases are also consistent with the initial magnetic linkage ideas of Néel and Gilleo. It is satisfying to see such agreement based on the theory for a randomly split d sublattice, since this is precisely the situation one would expect, based on the random canting description of Geller and co-workers.

Several comments on the comparison between theory and experiment under the assumption of zero d'–d' interaction are of importance. First, the initial approach of Yafet and Kittel was for split sublattices of a long-range nature. The ordered split proposed by de Gennes was in the spirit of that approach and entirely justified at the time. However, as pointed out by Geller and co-workers (see GWES and Geller (1978)), the predictions based on this condition fare poorly in comparison with data. The situation is evident from the lower broken line in figure 3, obtained with a J_{da}/J_{dd} ratio of 2.349 from GWES. Furthermore, under the de Gennes condition, the 'best fit' J_{da}/J_{dd} ratio near the data maximum in figure 4 is *double* the indicated values for $J_{d'a}/J_{d'd''}$. A J_{da}/J_{dd} ratio of 3.0–3.5 is well above the nominal range of values, 2–2.5 in table 3. With hindsight, at least in the opinion of these authors, the failure was more in the assumption of non-interacting d'–d' moments than in the basic model.

Figure 4 shows the experimental data points of GWES for Si- and Ge-substituted YIG. The site distributions of the various ions for Si-substituted YIG are taken to be $\{Y_{3-x}Ca_x\}[Fe_2](Fe_{3-x}Si_x)O_{12}$ and the same expression with Ge in place of Si for Ge-substituted YIG. In these cases, substitutions on the d sublattice initially reduce the net moment. For $x > 1.0$, the a-sublattice moment becomes larger than that of the d-sublattice. Canting comes in for $x \gtrsim 1.6$–2.0 as the intersublattice exchange becomes too weak to hold the a-site spins in alignment.

The full curves in figure 4 indicate theoretical predictions based on the present model for various choices of the $J_{a'd}/J_{a'a''}$ ratio, with q and n parameters appropriate for d-site substitutions in YIG. $q_a = 2$, $q_d = 3 - x$, $n_{ad} = 2(3 - x)$, $n_{dd} = 4(3 - x)/3$, $n_{aa} = 8$, and $n_{da} = 4$. The straight line in figure 4 was obtained from the Yafet–Kittel model with $J_{a'd}/J_{a'a''} = 5$. The broken line close to the horizontal axis will be discussed shortly. The comments for a-site-substituted YIG generally apply to these results as well. The linear dependences from Yafet–Kittel become somewhat more rounded, and the onset of canting is shifted to somewhat lower substituent concentrations for a given exchange ratio. As before, no single ratio gives a reasonable overall fit. The best fit near the data minimum is for $J_{a'd}/J_{a'a''} = 3$–4, which is generally consistent with the values in table 3.

The curves in figure 4 are much less rounded than the corresponding results of Rosencwaig (1970a).

Most of the comments of the last subsection with regard to the d'–d' and d'–d'' split sublattice interactions also apply here, but for a'–a' and a'–a''. The 'best fit' near the data minimum occurs for a $J_{a'd}/J_{a'a''}$ ratio in the 3–4 range. For a randomly split a sublattice, this implies a 'best fit' J_{ad}/J_{aa} ratio of 3–4 as well. This range compares favourably with the nominal values in the range 3–5 in table 3. The data for $x > 2.0$ in

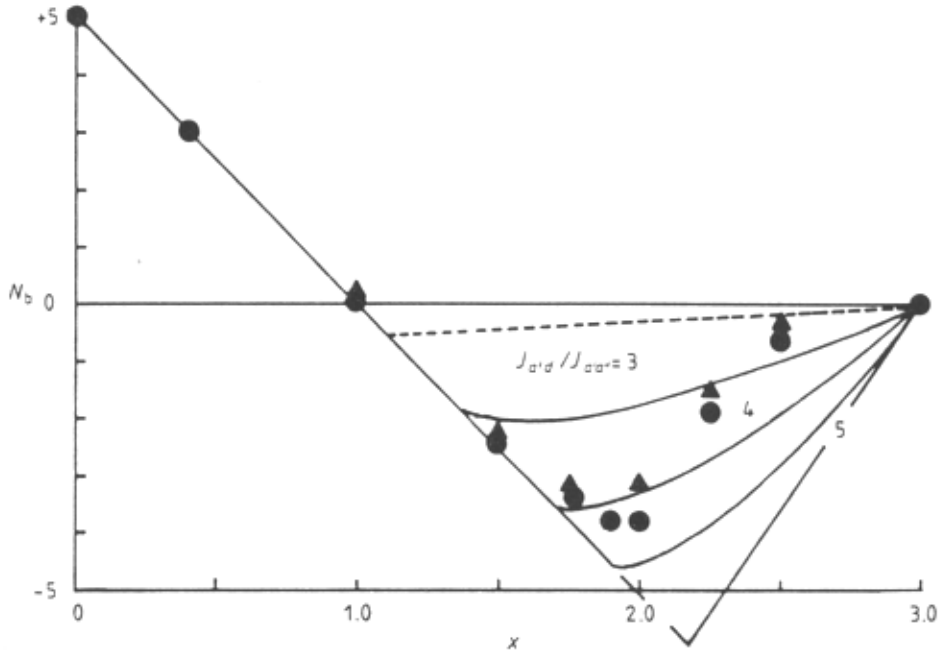

Figure 4. Comparison of theoretical predictions with data on the 0 K spontaneous moment of Si- and Ge-substituted YIG by Geller *et al* (1964). The moment N_b in μ_B per formula unit is shown as a function of substituent level x in $\{Y_{3-x}Ca_x\}[Fe_2](Fe_{3-x}M_x)O_{12}$ with M = Si (circles) and M = Ge (triangles).

figure 4, in comparison with the calculated curves, also indicate a decrease in the J_{ad}/J_{aa} ratio at high levels of d-sublattice substitution.

As was the case for a-sublattice substitutions, predictions based on either the Yafet–Kittel approach or the present model fare poorly under the assumption of zero a'–a' interaction. The broken line close to the x axis in figure 4 is based on a J_{ad}/J_{aa} ratio of 4.229 from GWES for zero a'–a' interaction. As pointed out by Geller and co-workers, this result is in drastic disagreement with the data. Conversely, zero a'–a' interaction would lead to a 'best fit' J_{ad}/J_{aa} ratio near the data minimum of figure 4 in the 6–8 range, substantially above the nominal 3–5 values in table 3.

Figure 5 shows experimental data points for the extrapolated zero field magnetisation at 4 K for zinc-substituted lithium ferrite, $(Zn_xFe_{1-x})_A[Li_{0.5-x/2}Fe_{1.5-x/2}]_BO_4$, as a function of zinc content in at./formula unit from $x = 0$ to $x = 1.0$. The magnetisation is in Bohr magnetons per formula unit. The actual data are similar to that of Patton *et al* (1982) except that careful extrapolations of the linear part of the high-field magnetisation curve (usually 20–40 kOe up to 80 kOe) to zero field were used to determine the spontaneous moments.

The full curves in figure 5 indicate theoretical predictions based on the present model

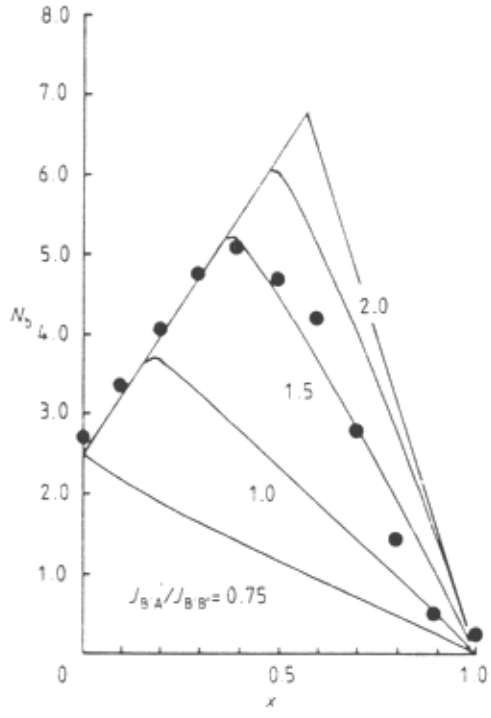

Figure 5. Comparison of theoretical predictions with data on the 4 K, extrapolated zero-field magnetisation of Li–Zn ferrite. The moment N_b in μ_B per formula unit is shown as a function of substituent level x in $(Zn_xFe_{1-x})[Li_{0.5-x/2}Fe_{1.5-x/2}]O_4$.

for various choices of $J_{B'A}/J_{B'B''}$, with q and n parameters appropriate for Li–Zn ferrite, $\langle n_{B'A}\rangle = 6(1-x)$, $\langle n_{AB'}\rangle = 3(1.5+x/2)$, $\langle n_{B'B''}\rangle = 3(1.5+x/2)/2$, $q_A = (1-x)$ and $q_{B'} = (1.5+x/2)/2$. Most of the comments for both of the substituted YIG examples are applicable to Li–Zn ferrite as well. The linear dependences from Yafet–Kittel become somewhat more rounded, but not extremely so. The iterative scheme yields a canting onset at somewhat lower substituent levels than from Yafet–Kittel, for the same exchange ratio. No single ratio gives a good overall fit, even though the lack of fit at $J_{B'A}/J_{B'B''} = 1.5$, for example, is not as bad as in the YIG examples.

The comments of the previous two subsections concerning split-sublattice interactions also apply here. The 'best fit' values of $J_{B'A}/J_{B'B''} \sim 1.3$–$1.5$ near the data maximum correspond to values of J_{BA}/J_{BB} of 1.3–1.5 as well, assuming a randomly split sublattice with $J_{BB} = J_{B'B'} = J_{B''B''}$. This ratio is somewhat lower than the values listed in table 4, and consistent with the previous indication of a decrease in the inter–intrasublattice exchange ratio with substitution.

The variations in the exchange integral ratio J_{BA}/J_{BB} as a function of zinc substitution,

Table 4. Literature values of the exchange constants J_{BA} and J_{BB}, and the ratio J_{BA}/J_{BB} for lithium ferrite, $Li_{0.5}Fe_{2.5}O_4$.

J_{BA} (K)	J_{BB} (K)	J_{BA}/J_{BB}	Reference
−32.9	−14.5	2.26	Rado and Folen (1960)
−34.1	−15.0	2.28	Dionne (1974)
−29.0	−8.0	3.63	Srivastava *et al* (1979)

obtained by fitting the curves in figure 5 to the data (assuming randomly split sublattices), are shown in figure 6 by the solid triangles; the circles represent similar fits based on the Yafet–Kittel model. Apart from the apparent downturn in the fitted values for 0.4 and 0.5 Zn at./formula unit, the trend appears to be reasonably consistent, as indicated by the broken line.

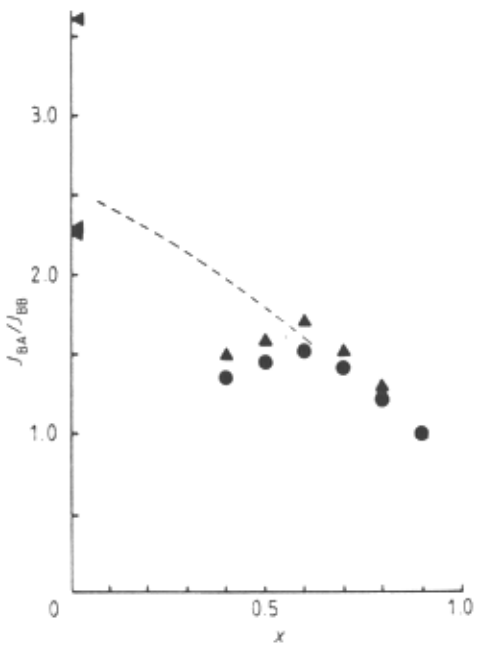

Figure 6. Fitted values of the exchange integral ratio J_{BA}/J_{BB} versus zinc level x in $(Zn_xFe_{1-x})[Li_{0.5-x}Fe_{1.5-x/2}]O_4$, using the data in figure 5. The triangles are for fits to the fully localised iterative model, based on the randomly split sublattice condition. The circles resulted from fits to the Yafet–Kittel model. The points along the vertical axis at $x = 0$ are from table 4.

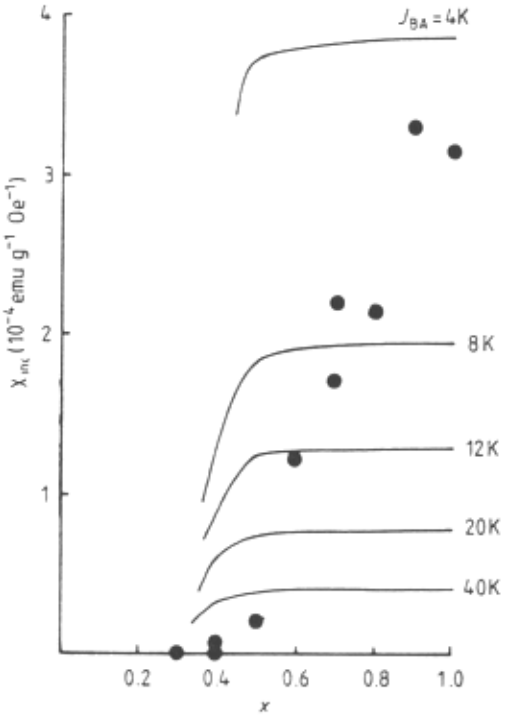

Figure 7. Comparison of the high-field incremental susceptibility χ_{inc} versus zinc level x in $(Zn_xFe_{1-x})[Li_{0.5-x}Fe_{1.5-x/2}]O_4$, obtained from the fully localised iterative model with the randomly split sublattice condition and $J_{BA}/J_{BB} = 1.5$, with data by Patton *et al* (1982).

We note that a similar downturn (but for larger J_{BA}/J_{BB} values) was obtained by Dionne (1974) by fitting the molecular-field theory to magnetisation versus temperature data for $0 < x < 0.3$. The origin and significance (if any) of these downturns are not clear at present.

A final point of comparison for the Li–Zn ferrite system is possible. Jacobs (1959a, b), Geller (1966, 1969) and White *et al* (1979) have used the existence of a high-field incremental susceptibility (e.g. lack of saturation in moderate fields) as an indication of non-collinear spins. The calculation described in §§ 2 and 3 is easily modified to include an applied field, which is simply added to the $H_{d'a}(m, x)$ in figure 2 and equation (20). With the field included, however, the magnitudes of the two individual exchange integrals, J_{da} and J_{dd} (or J_{ad} and J_{aa}, or J_{BA} and J_{BB}) enter the calculation as independent quantities, not just in ratio. Thus, susceptibility data can be used in combination with magnetisation data to determine values of the individual exchange parameters as well as ratios.

In figure 7, recent data by Patton *et al* (1982) are presented, along with a family of theoretical curves generated by the iterative, self-consistent procedure. Tne J_{BA}/J_{BB}

ratio was taken as 1.5, corresponding to the best rough fit in figure 5 (assuming randomly split sublattices), and the exchange integral J_{BA} was assigned the values indicated. There is a remarkable lack of agreement between the calculation and the data. The experimental susceptibility increases monotonically as soon as canting commences, above about 0.4 Zn at./formula unit. The theoretical curves behave quite differently. Once canting starts, the theoretical susceptibilities increase rapidly to some constant value which is independent of the zinc level for a given J_{AB}. This comparison is quite striking. It shows rather conclusively that a *constant, substitution-independent* exchange does *not* yield consistent theoretical fits to the experimental results for canting in substituted magnetic oxides.

Following the procedure used to obtain the fitted J_{BA}/J_{BB} ratios shown in figure 6, those ratios from figure 6 were combined with the susceptibility data of figure 7 to obtain fitted values of J_{BA} and J_{BB} as a function of zinc level. These fits indicate that dilution of one sublattice causes *both* of the pertinent exchange integrals as well as their ratio to decrease with level of substituent. Zinc levels above $x = 0.5$ are reasonably consistent with the literature values of the J_{BA} and J_{BB} exchange parameters (table 4) for pure Li ferrite, as well as recent spin-wave stiffness measurements in Li–Zn ferrite (Wilber *et al* 1983).

5. Conclusion

The foregoing has made it clear that a refined self-consistent iterative rendition of the localised canting calculation yields results which are significantly different from the earlier attempts at localised canting analyses. The curves of magnetisation versus substituent level are much less rounded than indicated by previous work and are, in fact, much closer to the simple Yafet–Kittel production than to the results of Rosencwaig.

However, the results do represent much more than simply a minimal improvement over Yafet–Kittel. They indicate that the effective exchange parameters must vary with the amount of non-magnetic substituent in the system. Fitting procedures applied to the three examples in § 4 yield exchange parameter ratios and, for Li ferrite, exchange parameters which are roughly consistent with reported values of the exchange constants for unsubstituted systems. In all three cases, substitution appears to cause a substantial decrease in the inter-intrasublattice exchange integral ratio for the higher levels of substitution at which canting effects become pronounced. The various comparisons tend to support a model interpretation in terms of randomly split sublattices, rather than in terms of non-interacting d'–d' and d''–d'' (or a'–a' and a''–a'', or B′–B′ and B″–B″) moments. In addition to the variation in the exchange ratio with substitution, high-field susceptibility data for the Li–Zn ferrite system allows the individual J_{BA} and J_{BB} integrals to be fitted versus zinc content. Both appear to decrease with zinc above about 0.5 Zn at./formula unit.

Acknowledgments

The authors are indebted to S Geller, G O White, G F Dionne, C A Edmondson, and S Kern for helpful discussions. Y H Liu was supported on an exchange program of the People's Republic of China. The work was supported in part by the United States Army Research Office, Contract No DAAG29-88K-0084, and the National Science Foundation, Grant No DMR-8013727.

Appendix 1. Yafet–Kittel model

The Yafet–Kittel molecular-field model applied to d-sublattice spin canting due to non-magnetic a sublattice substitutions in YIG, for example, utilises a split-sublattice magnetisation scheme the same as shown in figure 1 with the $\boldsymbol{S}$ vectors replaced by $\boldsymbol{M}$ vectors. The d sublattice is split into two half-sublattice magnetisations $\boldsymbol{M}_{d'}$ and $\boldsymbol{M}_{d''}$, each canted at an angle θ. The minority a sublattice has magnetisation $\boldsymbol{M}_a$ oriented antiparallel to the net d magnetisation, $\boldsymbol{M}_{d'} + \boldsymbol{M}_{d''}$, and the field $\boldsymbol{H}_0$. The pertinent molecular fields are as follows:

$$\boldsymbol{H}_a = \lambda_{aa}\boldsymbol{M}_a + \lambda_{ad'}\boldsymbol{M}_{d'} + \lambda_{ad''}\boldsymbol{M}_{d''}, \tag{A1.1a}$$

$$\boldsymbol{H}_{d'} = \lambda_{d'a}\boldsymbol{M}_a + \lambda_{d'd'}\boldsymbol{M}_{d'} + \lambda_{d'd''}\boldsymbol{M}_{d''}, \tag{A1.1b}$$

$$\boldsymbol{H}_{d''} = \lambda_{d''a}\boldsymbol{M}_a + \lambda_{d''d'}\boldsymbol{M}_{d'} + \lambda_{d''d''}\boldsymbol{M}_{d''}. \tag{A1.1c}$$

In the above, the λ_{ij} denote the molecular-field coefficients for the effective exchange field experienced by sublattice (or split sublattice) i due to the magnetisation of sublattice (or split sublattice) j. All molecular-field equations presented here are in terms of magnetic moment per formula unit, e.g. $Y_3Fe_5O_{12}$ etc. The free energy,

$$E = \tfrac{1}{2}[\boldsymbol{M}_a \cdot \boldsymbol{H}_a + \boldsymbol{M}_{d'} \cdot \boldsymbol{H}_{d'} + \boldsymbol{M}_{d''} \cdot \boldsymbol{H}_{d''}], \tag{A1.2}$$

is evaluated subject to the condition $M_{d''} = M_{d'}$, $\lambda_{ad'} = \lambda_{ad''} = \lambda_{d'a} = \lambda_{d''a}$, and $\lambda_{d'd''} = \lambda_{d''d'}$. Minimisation with respect to θ yields an expression for the Yafet–Kittel canting angle θ_{YK},

$$\cos\theta_{YK} = (2M_a\lambda_{d'a} + H_0)/4M_{d'}\lambda_{d'd''}, \tag{A1.3}$$

subject to $|\cos\theta_{YK}| \leq 1$. Equation (A1.3) for zero field is the same as case 2(a), p 291 in Yafet and Kittel (1952). The corresponding total magnetisation is given by $M = 2M_{d'}\cos\theta_{YK} - M_a$.

Appendix 2. Interpretation of split-sublattice molecular-field parameters

The above interpretation of the Yafet–Kittel model allows one to determine average canting angles for the split sublattice in terms of split-sublattice molecular-field coefficients $\lambda_{d'a}$ and $\lambda_{d'd''}$. The localised canting calculation described in the text allows one to obtain results in terms of split-sublattice exchange integrals $J_{d'a}$ and $J_{d'd''}$. Now, published data on exchange parameters are generally for the conventional two-sublattice parameters, $\lambda_{da}(=\lambda_{ad})$, λ_{aa}, λ_{dd} (or $J_{da} = J_{ad}$, J_{aa} and J_{dd}). In order to compare predictions of any canting model with data, a connection between parameters with primed and unprimed subscripts is needed.

One may obtain $\lambda_{d'd''}$ and $\lambda_{d'a}$ from empirical determinations of the molecular-field coefficients of the normal two-sublattice ferrimagnet, defined by $\boldsymbol{H}_a = \lambda_{aa}\boldsymbol{M}_a + \lambda_{ad}\boldsymbol{M}_d$, and $\boldsymbol{H}_d = \lambda_{da}\boldsymbol{M}_a - \lambda_{dd}\boldsymbol{M}_d$. To do so, however, it is necessary to make specific assumptions concerning $\lambda_{d'd''}$. This is evident from equation (A1.1b) for $\boldsymbol{M}_{d'} = \boldsymbol{M}_{d''} = \boldsymbol{M}_d/2$:

$$\boldsymbol{H}_d = \lambda_{d'a}\boldsymbol{M}_a + [(\lambda_{d'd'} + \lambda_{d'd''})/2]\boldsymbol{M}_d. \tag{A2.1}$$

It is clear that λ_{dd} is the *arithmetic mean* of $\lambda_{d'd'}$ and $\lambda_{d'd''}$.

This result is not new and, in fact, is contained in the original formulation by Yafet and Kittel, expressed by $\alpha_1 + \alpha_2 = 2\alpha$ and $\gamma_1 + \gamma_2 = 2\beta$ (Yafet and Kittel (1952), p 291). de Gennes (1959) adopted the view that a 'natural' split of the d sublattice into two parts would be such that d'-site spins would have only d''-site nearest neighbours. Implicit in this view is the existence of a true long-range order sublattice character for these hypothetical d' and d'' networks. The split therefore requires $\lambda_{d'd'} = 0$ and $\lambda_{d'd''} = 2\lambda_{dd}$, for nearest-neighbour interactions only. This assumption, while not explicitly stated, was used in obtaining numerical results from the Yafet–Kittel model for substituted YIG (Geller *et al* 1964, Geller 1966, 1969, 1978), as discussed in § 4. Within the spirit of the times, this interpretation may be viewed as reasonable. For d' and d'' spins to be *bona fide* members of genuinely separate sublattices (albeit split split sublattices), some ordered spatial arrangement would be necessary. The de Gennes condition $\lambda_{d'd'} = 0$ was simply a consequence of a particular arrangement.

It is now generally accepted, however, that the random substitutions on the a sublattice, for example, lead to a canting of d-site moments which depends on the specifics of the particular d-site nearest-neighbour environment. This canting is not ordered but is random, in the same sense that the distribution of ions within the substituted sublattice is random (Geller *et al* 1964, Geller 1966, 1969). It is a simple extension to argue that, on a spin-for-spin basis, the split of spins between the two sub-sublattices, albeit artificial, would also be random. A given spin would 'see' equal molecular-field coefficients due to each of the two split sublattices. As a consequence, $\lambda_{d'd'} = \lambda_{d'd''}$, and $\lambda_{dd} = \lambda_{d'd''}$ are satisfied. In the comparisons presented in § 4 both possibilities are considered.

Appendix 3. Relation of molecular-field coefficients to exchange integrals

Exchange interactions are generally expressed in terms of molecular-field coefficients, as used in the preceeding parts of this Appendix, or in terms of the J_{ij} exchange integrals used in the body of this paper. It is not generally true that the ratios of various λs are the same as the ratios of their counterpart Js. In order to have consistent relations between λ coefficients and the J parameters, as well as the various ratios, a conversion recipe is needed.

Considering YIG in the two sublattice approximation, the free energy from equation (1) for zero field is

$$E = +|J_{aa}|q_a n_{aa} S^2 - |J_{ad}|q_a n_{ad} S^2 - |J_{ad}|q_d n_{da} S^2 + |J_{dd}|q_d n_{dd} S^2, \tag{A3.1}$$

where q_a and q_d denote the numbers of a- and d-site magnetic ions per formula unit and n_{ad} etc denote the number of nearest-neighbour d-site magnetic ions to an a site, etc. The molecular-field approach, based on fields as in Appendix 2 and an energy (following Yafet–Kittel) $E = \frac{1}{2}(\boldsymbol{H}_a \cdot \boldsymbol{M}_a + \boldsymbol{H}_d \cdot \boldsymbol{M}_d)$, where $M_{a,d} = q_{a,d}(g\mu_B S)$, leads to the following relations between the λs and Js:

$$|\lambda_{aa}| = (2n_{aa}/q_a)|J_{aa}|/(g\mu_B)^2, \tag{A3.2a}$$

$$|\lambda_{dd}| = (2n_{dd}/q_d)|J_{dd}|/(g\mu_B)^2, \tag{A3.2b}$$

$$|\lambda_{da}| = [(q_a n_{ad} + q_d n_{da})/q_a q_d]|J_{da}|/(g\mu_B)^2. \tag{A3.2c}$$

These relations will be used in making comparisons between theory and data in § 4. We note that for pure YIG there is no distinction between average and local nearest-

neighbour parameters. Furthermore, the above relations between the λs and Js are valid for parameters with primed subscripts.

References

Aléonard R 1960 *J. Phys. Chem. Solids* **15** 167
Anderson E E 1964 *Phys. Rev.* **134** A1581
Anderson P W 1956 *Phys. Rev.* **102** 1008
Dickof P A, Schurer P J and Morrish A H 1980 *Phys. Rev.* B **22** 115
Dionne G F 1970 *J. Appl. Phys.* **41** 4874
—— 1974 *J. Appl. Phys.* **45** 3621
Douglass R L 1960 *Phys. Rev.* **120** 1612
Geller S 1960 *J. Phys. Chem. Solids* **16** 21
—— 1966 *J. Appl. Phys.* **37** 1408
—— 1969 *Phys. Rev.* **181** 980
—— 1978 *Physics of Magnetic Garnets* (Bologna: Tipografia Compositori) pp 1–55
Geller S, Williams H J, Espinosa G P and Sherwood R C 1964 *Bell Syst. Tech. J.* **63** 565
Geller S, Williams H J, Sherwood R C and Espinosa G P 1962 *J. Appl. Phys.* **33S** 1195
de Gennes P G 1959 *Phys. Rev. Lett.* **3** 209
Gilleo M A 1958 *Phys. Rev.* **109** 777
—— 1960 *J. Phys. Chem. Solids* **13** 33
Gilleo M A and Geller S 1958 *Phys. Rev.* **110** 73
Gonano R, Hunt E and Meyer H 1967 *Phys. Rev.* **156** 521
Gorter E W 1950 *C.R. Acad. Sci., Paris* **230** 192
Guillaud C and Creveaux H 1950 *C.R. Acad. Sci., Paris* **230** 1458
Guillaud C and Roux M 1949 *C.R. Acad. Sci., Paris* **228** 1110
Harris A B 1963 *Phys. Rev.* **132** 2398
Jacobs I S 1959a *J. Phys. Chem. Solids* **11** 1
—— 1959b *J. Appl. Phys.* **30** 301S
Kaplan T A 1959 *Phys. Rev.* **116** 888
—— 1960 *Phys. Rev.* **119** 1460
Lotgering F K 1956 *Philips Res. Rep.* **11** 190
Morrish A H 1981 *Ferrites—Proc. ICF3* ed. H Watanabe, S Iida and M Sugimoto (Tokyo: Center for Academic Publications, Japan) p 153
Néel L 1948 *J. Phys. Rad.* **9** 184
—— 1950 *C.R. Acad. Sci., Paris* **230** 375
Nowik I 1968 *Phys. Rev.* **171** 550
—— 1969a *J. Appl. Phys.* **40** 872
—— 1969b *J. Appl. Phys.* **40** 5184
Patton C E, Edmondson C A and Liu Y H 1982 *J. Appl. Phys.* **53** 2431
Pauthenet R 1958 *Ann. Phys., Paris* **3** 424
Rado G T and Folen V J 1960 *J. Appl. Phys.* **31** 62
Rosencwaig A 1970a *Can. J. Phys.* **48** 2857
—— 1970b *Can. J. Phys.* **48** 2868
Solt I H 1962 *J. Appl. Phys.* **33** 1189
Srivastava C M, Srinivasan G and Nanadikar N G 1979 *Phys. Rev.* B **19** 499
Verwey E J W and Heilmann E L 1947 *J. Chem. Phys.* **15** 174
White G O, Edmondson C A, Goldfarb R B and Patton C E 1979 *J. Appl. Phys.* **50** 2381
Wilber W, Kabos P and Patton C E 1983 *IEEE Trans. Magn.* **19** in press
Winkler G 1981 *Magnetic Garnets* (Braunschweig: Vieweg)
Wojtowicz P J 1964 *Phys. Lett.* **11** 18
Yafet Y and Kittel C 1952 *Phys. Rev.* **87** 290